THE JOURNAL OF BIOLOGICAL CHEMISTRY Vol. 278, No. 1, Issue of January 3, pp. 194–199, 2003

Printed in U.S.A.

A Nucleophilic Catalysis Step is Involved in the Hydrolysis of Aryl Phosphate Monoesters by Human CT Acylphosphatase*

Received for publication, July 11, 2002, and in revised form, October 28, 2002
Published, JBC Papers in Press, October 29, 2002, DOI 10.1074/jbc.M206918200

Paolo Paoli, Luigia Pazzagli, Elisa Giannoni, Anna Caselli, Giampaolo Manao, Guido Camici‡, and Giampietro Ramponi

From the Department of Biochemical Sciences, University of Florence, Viale Morgagni 50, 50134 Florence, Italy

Acylphosphatase, one of the smallest enzymes, is expressed in all organisms. It displays hydrolytic activity on acyl phosphates, nucleoside di- and triphosphates, aryl phosphate monoesters, and polynucleotides, with acyl phosphates being the most specific substrates *in vitro*. The mechanism of catalysis for human acylphosphatase (the organ-common type isoenzyme) was investigated using both aryl phosphate monoesters and acyl phosphates as substrates. The enzyme is able to catalyze phosphotransfer from *p*-nitrophenyl phosphate to glycerol (but not from benzoyl phosphate to glycerol), as well as the inorganic phosphate-$H_2{}^{18}O$ oxygen exchange reaction in the absence of carboxylic acids or phenols. In short, our findings point to two different catalytic pathways for aryl phosphate monoesters and acyl phosphates. In particular, in the aryl phosphate monoester hydrolysis pathway, an enzyme-phosphate covalent intermediate is formed, whereas the hydrolysis of acyl phosphates seems a more simple process in which the Michaelis complex is attacked directly by a water molecule generating the reaction products. The formation of an enzyme-phosphate covalent complex is consistent with the experiments of isotope exchange and transphosphorylation from substrates to glycerol, as well as with the measurements of the Brønsted free energy relationships using a panel of aryl phosphates with different structures. His-25 involvement in the formation of the enzyme-phosphate covalent complex during the hydrolysis of aryl phosphate monoesters finds significant confirmation in experiments performed with the H25Q mutated enzyme.

Acylphosphatase (ACP),[1] one of the smallest enzymes (11 kDa), is expressed in all known organisms, and its cellular function has not been hitherto fully understood. Several reports indicate that ACP is involved in controlling membrane ion pumps (Refs. 1 and 2 and citations therein) because *in vitro* it displays hydrolytic activity against the aspartyl phosphate intermediate formed during the action of membrane Na^+,K^+- and Ca^{2+}-ATPases. The fact that ACP is able to bind sarco-/endoplasmic reticulum calcium ATPase (3) is in line with the preceding hypothesis. Other reports note the involvement of ACP in cell differentiation and apoptosis (4–6); the ACP level is greatly enhanced during the differentiation process that a number of specific compounds (triiodothyronine, phorbol 12-myristate 13-acetate, aphidicolin, and hemin) induce, and moreover, the enzyme is able to migrate into the nucleus during both differentiation and apoptosis (7, 8). The overexpression of ACP in yeast cells enhances the rate of glycolysis, suggesting that it is capable of hydrolyzing 1,3-bisphosphoglycerate *in vivo* (9).

Site-directed mutagenesis experiments suggest that Arg-23 and Asn-41 are essential residues (10, 11), Arg-23 being involved in the binding of the substrate phosphate moiety (12). A model based on x-ray crystallography data for the catalytic hydrolysis of acyl phosphates by ACP was previously proposed by Thunnissen *et al.* (12).

In this article we demonstrate that human CT acylphosphatase catalyzes the hydrolysis of aryl phosphates displaying a different mechanism from the one it uses for acyl phosphate hydrolysis. For *p*-nitrophenyl phosphate hydrolysis, we found that the enzyme uses His-25 to perform a nucleophilic catalysis step, which, by contrast, it does not use in the catalytic hydrolysis of acyl phosphates.

EXPERIMENTAL PROCEDURES

Reagents—Benzoyl phosphate was synthesized as described previously (13). The aryl phosphate monoesters 4-cyano and 3-chloro were synthesized as dicycloexylammonium salts in accordance with Zhang and Van Etten (14), whereas *p*-nitrophenyl phosphate, phenyl phosphate, β-naphtyl phosphate, and L-tyrosine phosphate where purchased from Sigma. [^{18}O]water at 97% isotope enrichment was purchased from Cambridge Isotope Laboratories. All other reagents were the purest commercially available grade.

Enzymes—wild-type human CT-ACP was produced and purified as previously described (15). The H25Q mutant of CT-ACP was obtained by oligonucleotide-directed mutagenesis using a unique site elimination (USE) mutagenesis kit based on the USE method developed by Deng and Nickoloff (16). The mutations were confirmed by DNA sequencing according to Sanger *et al.* (17) and by amino acid analysis of the purified proteins.

Determination of Enzyme Activity—Benzoylphosphatase activity was assayed using a continuous optical test in accordance with Ramponi *et al.* (18). The hydrolytic activity on aryl phosphates was in general assayed as follows: substrates were dissolved in 1 ml of 0.1 M acetate buffer, pH 5.3, containing 1 mM EDTA (Buffer 1). The mixture was incubated at 37 °C and after the addition of the enzyme, aliquots were taken at different times to assay the released P_i by the method of Baginski *et al.* (19). The *p*-nitrophenyl phosphatase activity was assayed at 37 °C; pNPP was dissolved in Buffer 1 at the final volume of 1 ml. The reaction was stopped by the addition of 4 ml of 0.1 M KOH, and the released *p*-nitrophenolate ion was measured at 400 nm (ϵ = 18,000 $M^{-1}cm^{-1}$).

Inorganic Phosphate-Water Medium ^{18}O Exchange—An orthophosphoric acid solution (100 mM final concentration) was adjusted to pH 5.3

* This work was funded in part by the Consiglio Nazionale delle Ricerche (CNR Target Project on Biotechnology) and in part by the Ministero dell'Istruzione, dell'Università e della Ricerca (MIUR-CNR, Biotechnology Program L.95/95). The costs of publication of this article were defrayed in part by the payment of page charges. This article must therefore be hereby marked "*advertisement*" in accordance with 18 U.S.C. Section 1734 solely to indicate this fact.

‡ To whom correspondence should be addressed: Dipartimento di Scienze Biochimiche, Università degli Studi di Firenze, Viale Morgagni 50, 50134 Firenze, Italy. Tel.: 39-055-413765; Fax: 39-055-4222725; E-mail: camici@scibio.unifi.it.

[1] The abbreviations used are: ACP, acylphosphatase; CT, organ-common type isoenzyme; pNPP, *p*-nitrophenyl phosphate; pNP, *p*-nitrophenol; *E*-P, enzyme-phosphate; MS, mass spectrometry.

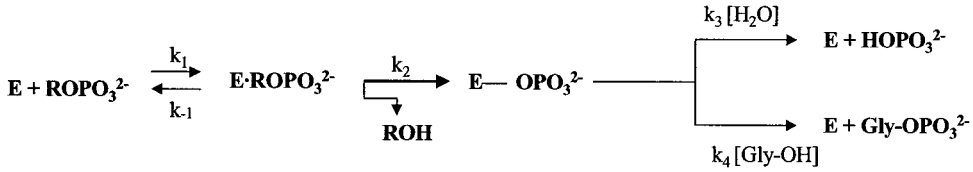

SCHEME 1. ***E*, enzyme; *R*, aryl or acyl; *ROH*, phenol or carboxylic acid; *Gly-OH*, glycerol.**

with NaOH. Then, 25 μl were withdrawn and transferred to a small screw-cap conical vial and dried. The residue was dissolved in 25 μl of [^{18}O]water, and 1 μl of human CT-ACP (0.28 g/liter) was added. The mixture was incubated at room temperature. Aliquots of 2 μl were withdrawn at varying incubation times and diluted with water to 100 μl in order to perform MS analyses. To verify the performance of the method, a parallel experiment with calf intestine alkaline phosphatase was carried out (in this experiment, the pH of the incubation mixture (25 μl) was adjusted to 9.0, and 0.14 units of alkaline phosphatase were added (the unit is defined as the amount of enzyme that catalyzes the hydrolysis of 1 μmol of pNPP at 25 °C and pH 9.0)).

Mass Spectrometry—Electrospray mass spectra in negative ion mode were obtained under the following conditions: ion spray voltage, 2.2 kV; nozzle potential, 120 V; quadrupole DC potential, 8.5 V; quadrupole rf potential, 350 V. Analyzer settings: push pulse potential, 770 V; pull pulse potential, 250 V; pull bias potential, 11.5 V; acceleration potential, 4 kV; reflector potential, 1.5 kV; detector potential, 2.05 kV. Scan range *m/z*, 60–300; scan rate, 8 ms/atomic mass.

RESULTS

Human CT-ACP Catalyzes the Transfer of Phosphate from pNPP to Glycerol but Not from Benzoyl Phosphate—The ability of ACP to catalyze phosphate transfer was verified by partition experiments using two different substrates, pNPP and benzoyl phosphate. Wild-type enzyme was added to Buffer 1 solution containing pNPP or, alternatively, benzoyl phosphate either in the presence or absence of 1 M glycerol, a nucleophile that may compete with water in attacking the phosphorus atom of the hypothesized *E*-P covalent intermediate (see Scheme 1).

At the appropriate times, aliquots of the mixtures were drawn off, and measurements were taken of the quantities of P_i and pNP or P_i and benzoate released. The overall rates of substrate turnovers (hydrolysis plus substrate transfer) were measured by the quantity of pNP or benzoate (from pNPP or benzoyl phosphate, respectively) produced, whereas the hydrolysis rates were measured by the quantity of inorganic phosphate produced. Table I shows that, in the absence of glycerol, the hydrolysis rates of pNPP or benzoyl phosphate, determined by the pNP or benzoate assays, were very close to those determined by the phosphate assays. In the presence of 1 M glycerol, we observed an increase in pNPP but not of benzoyl phosphate overall turnover. Table I shows the molar ratios of pNP/P_i produced by the ACP catalysis; at pH 5.3 and 6.5 they were, respectively, 0.97 and 0.94 in water, and 1.77 and 1.97 in 1 M glycerol. Table I also shows the results of experiments carried out with benzoyl phosphate; at pH 5.3, we found the benzoate/P_i molar ratio in water to be 1.01 and, in the water-glycerol mixture, 0.96, whereas at pH 6.5, we found it to be 1.0 in water and 0.97 in 1 M glycerol.

Glycerol Interacts with and Activates ACP—On measuring the fluorescence emission spectra of ACP at varying concentration of glycerol, we found that a higher glycerol concentration causes both a small drop of the signal and a small red-shift of the tryptophan emission band (Fig. 1*A*). ΔF increases hyperbolically in the range 0–0.2 M glycerol, suggesting that ACP binds glycerol. In the range 0–0.32 M glycerol, data fit well to the following equation (Fig. 1*B*),

$$\Delta F = \frac{\Delta F_{max}[\text{Gly-OH}]}{K_G + [\text{Gly-OH}]} \qquad \text{(Eq. 1)}$$

where K_G is the dissociation constant of the enzyme-glycerol complex, ΔF_{max} is the maximum value of ΔF, and Gly-OH indicates glycerol. This enables us to calculate a K_G value of 17 ± 1 mM.

The plot of k_{cat}/K_m against glycerol concentration (Fig. 1*C*) also shows hyperbolic behavior. Data fitting to the following equation (Fig. 1*C*),

$$\frac{k_{cat}}{K_m} = \frac{K'[\text{Gly-OH}]}{K_G + [\text{Gly-OH}]} \qquad \text{(Eq. 2)}$$

where K' is the size of the hyperbolic increase of k_{cat}/K_m due to glycerol binding and K_G indicates the dissociation constant of the enzyme-glycerol complex, gives K_G = 15 ± 4 mM, a value close to that calculated from fluorescence.

To assess the effect of glycerol on k_{cat}, we derived the overall k_{cat} of pNPP turnover from Scheme 1 (20, 21) as follows.

$$k_{cat} = \frac{k_2(k_3 + k_4[\text{Gly-OH}])}{k_2 + k_3 + k_4[\text{Gly-OH}]} \qquad \text{(Eq. 3)}$$

When the rate-limiting step is the hydrolysis or alcoholysis of *E*-P, Equation 3 can be reduced as follows.

$$k_{cat} = k_3 + k_4[\text{Gly-OH}] \qquad \text{(Eq. 4)}$$

Although the model described in Equation 4 indicates a linear correlation between k_{cat} and the concentration of glycerol, Fig. 1*D* shows that the data agree with a biphasic increase of k_{cat}, the initial phase (0–0.2 M glycerol) being hyperbolic and the secondary linear. Thus, the data fit Equation 5 quite well,

$$k_{cat(obs)} = \frac{k''[\text{Gly-OH}]}{K_G + [\text{Gly-OH}]} + (k_3 + k_4[\text{Gly-OH}]) \qquad \text{(Eq. 5)}$$

where k'' is the size of the hyperbolic increase of k_{cat} caused by glycerol binding, K_G is the dissociation constant of the enzyme-glycerol complex, and k_4 is the rate constant for alcoholysis of *E*-P (Scheme 1). From the k_{cat} data we calculate a K_G of 74 ± 15 mM, a value that is about 5-fold higher than that calculated from the data of fluorescence and k_{cat}/K_m. Considering that k_{cat}/K_m is the apparent second-order constant for the reaction of free enzyme and free substrate and that k_{cat} is the first order kinetic constant for the hydrolysis of the *E*-P covalent complex, the difference in the value of K_G indicates that the free enzyme binds glycerol more strongly than the *E*-P complex does.

The second-order rate constant (k_4) for phosphotransfer and the *E*-P hydrolysis constant (k_3) can be determined from Equation 5 (Fig. 1*D*). We found that k_4 = 0.10 ± 0.01 $M^{-1}s^{-1}$ and k_3 = 0.11 ± 0.01 s^{-1}. The ratio of the rate of phosphotransfer (k_4) to the rate of hydrolysis ($k_3' = k_3/[H_2O]$ (Scheme 1) is 50.5. This value, compared with those of other phosphatases forming *E*-P covalent intermediates in their catalytic pathways (21), indicates a moderate tendency of ACP to catalyze phosphotransfer.

The results of the fluorimetry experiments performed at low glycerol concentration demonstrate that glycerol interacts with the enzyme causing a hyperbolic increase of the overall activity. Nevertheless, at glycerol concentrations above 0.2 M, the linear increase of activity agrees with the fact that alcoholysis competes with hydrolysis for the *E*-P breakdown (Scheme 1).

Inorganic Phosphate-$H_2{}^{18}O$ Oxygen Exchange Experiments—

TABLE I

Partition experiments with wild-type and H25Q mutant of CT acylphosphatase

Experiments were performed at 37 °C in 0.1 M sodium acetate buffer, pH 5.3, and 0.1 M sodium cacodylate buffer, pH 6.5. Reactions were started by adding the appropriate amount of enzyme. At varying times, aliquots were withdrawn to assay, respectively, the released P_i and p NP for pNPP experiments and P_i and benzoate for benzoyl phosphate experiments. R-OH indicates *p*-nitrophenol or benzoate released from pNPP or benzoyl phosphate (B-P), respectively. wt, wild type. Experiments were performed with 2 mM B-P and 10 mM pNPP.

	pH 5.3			pH 6.5		
	B-P wt	pNPP wt	pNPP H25Q	B-P wt	pNPP wt	pNPP H25Q
Rate of R-OH production[a]						
in water	9816	0.567	0.103	2662	0.563	0.104
in 1 M glycerol	9369	1.166	0.142	2434	1.114	0.129
Rate of phosphate production[a]						
in water	9757	0.584	0.107	2656	0.602	0.101
in 1 M glycerol	9772	0.660	0.156	2518	0.565	0.126
Rate of phosphate transfer[a]	0	0.506	0	0	0.549	0
[R-OH]/[phosphate]						
in water	1.01	0.97	0.96	1.00	0.94	1.03
in 1 M glycerol	0.96	1.77	0.91	0.97	1.97	1.02
Transfer/hydrolysis ratio	0	0.77	0	0	0.97	0

[a] Values are expressed as μmol/min/mg of protein.

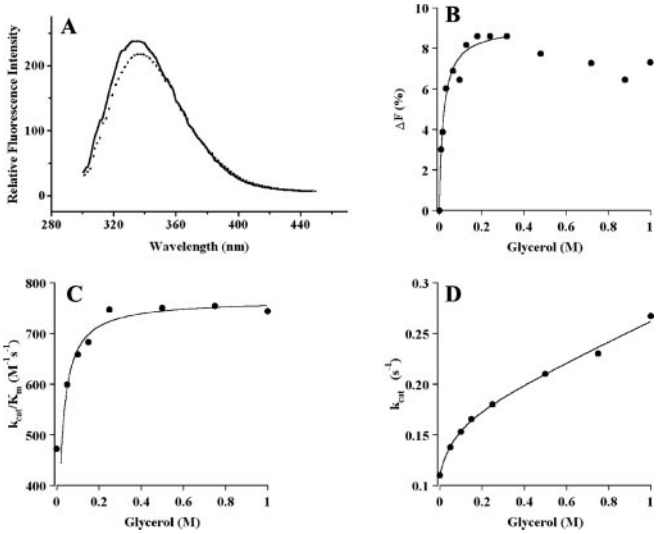

FIG. 1. **The effects of glycerol concentration on the fluorescence emission of human CT-ACP and on its main kinetic parameters.** *A*, fluorescence emission spectra of human CT-ACP in the absence and presence of glycerol. Spectra were acquired with a Shimadzu model RF-5000 spectrofluorimeter; the excitation wavelength was 280 nm. *Continuous line*, without glycerol; *dashed line*, with 0.3 M glycerol. The enzyme was dissolved in 0.1 M acetate buffer, pH 5.3, containing 0.15 M NaCl. In *B*, the experimental points indicate the relative difference of the fluorescence emission signal at 335 nm as a function of glycerol concentration. *C*, plot of k_{cat}/K_m *versus* glycerol concentration; *D*, plot of k_{cat} *versus* glycerol concentration. The initial rates of pNPP hydrolysis at the indicated glycerol concentrations were determined at pH 5.3 and 37 °C.

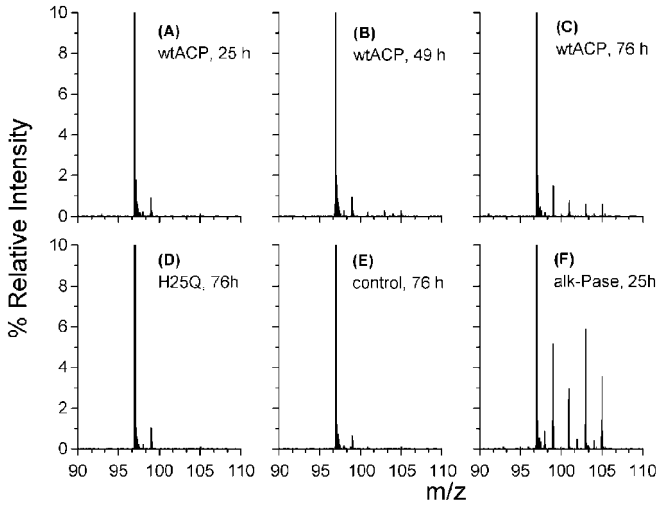

FIG. 2. **Electrospray MS-spectra from inorganic phosphate-$H_2{}^{18}O$ oxygen exchange experiments.** The panels show the intensities of ions relative to that of the $H_2P^{16}O_4^-$ isotopomer, for which intensity was fixed at 100%. The incubation times are indicated in the panels. *wt*, wild type.

Enzyme-catalyzed ^{18}O exchange between P_i and water was observed in a number of enzyme such as acid and alkaline phosphatases, ATPases, low M_r phosphotyrosine protein phosphatase, and the catalytic domain of leukocyte antigen-related phosphotyrosine protein phosphatase (Ref. 22 and citations therein). All of these enzymes indeed form a phosphoenzyme in their pathways. ^{18}O exchange is therefore a convenient technique for tracing *E*-P covalent complex formation in an enzymatic pathway. Human CT-ACP is able to catalyze the inorganic phosphate-$H_2{}^{18}O$ oxygen exchange reaction (Fig. 2). Experiments were performed at 25 °C and pH 5.3. MS spectra of control samples to which no enzyme was added confirm that the spontaneous exchange reaction was negligible (Fig. 2*E*). Fig. 2, *A–C*, shows the MS spectra of the mixtures containing wild-type ACP measured at 25, 49, and 76 h and demonstrates that the enzyme is able to catalyze the time-dependent incorporation of ^{18}O atoms into phosphate when incubated with unlabeled P_i and $H_2{}^{18}O$ in the absence of *p*-nitrophenol. All possible isotopomers are clearly present after 76 h of incubation. Taking into account the preceding results, we deduce that, in the presence of the enzyme and in the absence of phenols, the inorganic phosphate-$H_2{}^{18}O$ oxygen exchange can occur only if an *E*-P covalent intermediate is formed and then hydrolyzed by cycling the two terminal steps in the overall catalytic process shown in Scheme 2.

Fig. 2*F* illustrates the MS spectrum of an experiment performed with alkaline phosphatase, an enzyme that forms an *E*-P covalent intermediate in its catalytic pathway (23). This experiment, which shows the rapid incorporation of all oxygen isotopomers into phosphate, is a good control on the performance of the technique used here.

Structure-Activity Relationships—The initial rates for the ACP-catalyzed hydrolysis of six aryl phosphates differing in the leaving group pK_a values (phenyl phosphate, 4-cyanophenyl phosphate, 3-chlorophenyl phosphate, 4-nitrophenyl phosphate, β-naphthyl phosphate, and L-phosphotyrosine) were determined. Measurements were performed at pH 5.3 and 37 °C using the concentration range 0.05–3.2 mM for all substrates tested.

The V_{max} and K_m values were obtained by solving the Michaelis-Menten equation $v = V_{max}[S]/(K_m + [S])$ by nonlinear regression analysis with the aid of a computer program (Fig. P, BioSoft). We examined the effect of the leaving group

SCHEME 2. **The overall catalytic pathway of aryl phosphate monoester hydrolysis by human CT-ACP.** *E*, enzyme; *Ar*, aryl; *P*, phosphate group.

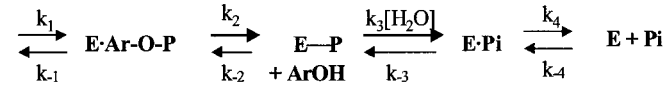

pK_a (pK_a range, 7.14–10.07) on k_{cat} and k_{cat}/K_m regarding the aryl phosphatase activity of ACP (Brønsted correlation). These free energy relationships provide information about the rate-limiting step of the catalytic process and the nature of the transition state. Fig. 3 shows the Brønsted plots that correlate, respectively, k_{cat} and k_{cat}/K_m values to the pK_a values of the substrate leaving group. The left side of this figure shows the findings of earlier experiments on k_{cat} and k_{cat}/K_m dependence on the leaving group of seven acyl phosphates (24), whereas the right side shows the results obtained here for k_{cat} and k_{cat}/K_m dependence on the leaving group pK_a of six aryl phosphates. For aryl phosphates, we found that the dependence of both log k_{cat} and log k_{cat}/K_m on the leaving group pK_a are monophasic (Fig. 3, *right*). By fitting the data to the linear equations

$$\log k_{cat} = \beta_{lg} pK^{XOH} + \text{constant} \quad \text{(Eq. 6)}$$

or

$$\log k_{cat}/K_m = \beta_{lg} pK^{XOH} + \text{constant} \quad \text{(Eq. 7)}$$

where pK is the pK_a of the leaving group XOH, we calculated, respectively, the β_{lg} values for k_{cat} (-0.07 ± 0.02) and k_{cat}/K_m (-0.20 ± 0.11). The very small dependence of k_{cat} and k_{cat}/K_m on the leaving group pK_a for aryl phosphates contrasts with the strong dependence of k_{cat} and k_{cat}/K_m on the leaving group pK_a for acyl phosphates ($\beta_{lg} = -1.38 \pm 0.14$, and $\beta_{lg} = -1.44 \pm 0.22$, respectively (see *left side* of Fig. 3, which shows data for the strictly homologous bovine enzyme; taken from Paoli *et al.* (24)). For aryl phosphates, the small dependence of k_{cat} on the structures of leaving group, which differ markedly in the pK_a (7.14 for 4-nitrophenyl phosphate and 10.07 for phosphotyrosine) indicates that the k_{cat} values for various aryl phosphates are very close to each other, suggesting that a common intermediate complex is formed and accumulated before the limiting step of the catalytic process takes place. No such accumulation of intermediate complex can be seen from the data relative to the hydrolysis of acyl phosphates catalyzed by the bovine CT-ACP (24), which is about 90% identical in sequence with the human CT acylphosphatase.

His-25 Is Involved in the Phosphotransfer and the Inorganic Phosphate-$H_2{}^{18}O$ Oxygen Exchange Reactions Catalyzed by ACP—Previous experiments have demonstrated that human CT-ACP was inactivated by the Woodward reagent K, which reacts specifically with His-25 located in the active site region, even though the enzyme contains other histidine residues and also several acidic residues that are potential targets for this reagent (25). This finding revealed a very reactive nucleophile in the active site region. We thus performed partition experiments with the H25Q mutant of human CT-ACP in the presence and absence of 1 M glycerol. Table I shows that the mutation of His-25 to Gln eliminates the enzyme capacity to catalyze the phosphotransfer reaction. Interestingly, as observed in the wild-type ACP, 1 M glycerol enhances the activity of the H25Q mutant (by ~40% at pH 5.3 and ~25% at pH 6.5), suggesting that the presence of glycerol also causes structural modifications to occur in this mutant. Furthermore, Fig. 2*D* shows that the mutation of His-25 to Gln in ACP causes a strong decrease in the catalytic rate of the inorganic phosphate-$H_2{}^{18}O$ oxygen exchange reaction. Taken together, all of these results suggest that His-25 is involved in the formation of an enzyme phosphohistidine intermediate during the catalytic hydrolysis of pNPP.

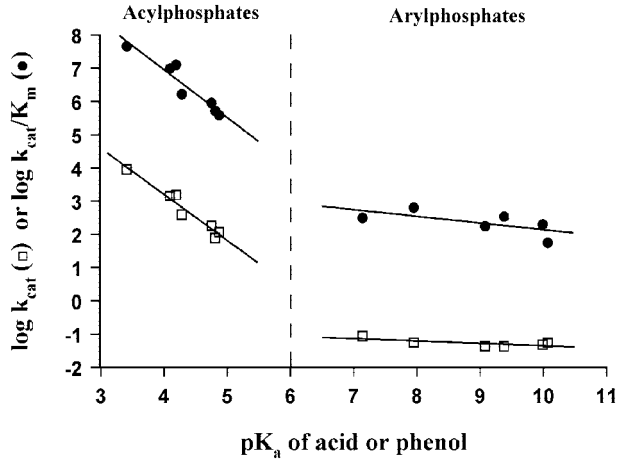

FIG. 3. **Effect of leaving group pK_a on k_{cat} and k_{cat}/K_m regarding CT acylphosphatase.** The lines were drawn using a linear regression method. Data for aryl phosphates are reported on the *right*; the experimental points refer to 4-nitrophenyl phosphate (7.14), 4-cyanophenyl phosphate (7.95), 3-chlorophenyl phosphate (9.08), β-naphtyl phosphate (9.24), phenyl phosphate (9.99), and L-phosphotyrosine (10.07). Data for acyl phosphates are shown on the *left*. The experimental points are taken from Paoli *et al.* (30) and refer to bovine CT-ACP, which has about 90% sequence identity with respect to the human enzyme. The pK_a value for each leaving group is indicated in parentheses.

DISCUSSION

Our results show evidence that human CT acylphosphatase catalyzes the hydrolysis of aryl phosphate monoesters by a mechanism that involves a nucleophilic catalysis step. On the contrary, no nucleophilic catalysis occurs in the enzymatic hydrolysis of acyl phosphates. We obtained consistent proof of our conclusions. First, the results obtained by kinetic experiments performed at both pH 5.3 and 6.5 in the presence and absence of glycerol suggest that an *E*-P covalent intermediate is formed during the catalytic hydrolysis of pNPP but not of benzoyl phosphate (see Table I). These findings also suggest that the hydrolysis of *E*-P is the limiting step of pNPP hydrolysis by CT-ACP. In fact, if the rate-limiting step is the formation of *E*-P (Scheme 1) and the acceptor reacts with the intermediate after the rate-limiting step, it does not increase the overall rate of pNPP breakdown. Only if the rate-limiting step is the hydrolysis of *E*-P, will the addition of the acceptor nucleophile increase the breakdown of the intermediate and hence enhance the overall reaction rate (14, 20). Furthermore, the results of experiments performed at increasing glycerol concentrations (range, 0.2–1 M) agree with the model described in Scheme 1 and Equation 4; this model assumes that an *E*-P covalent intermediate is formed in the catalytic pathway of aryl phosphate hydrolysis. In the 0–0.2 M glycerol concentration range, fluorescence spectroscopy shows that glycerol interacts with the enzyme and enhances its activity (see Fig 1). We also demonstrate that the mutation of His-25 to Gln completely eliminates the capacity of the enzyme to catalyze the transphosphorylation from pNPP to glycerol (Table I) demonstrating that His-25 is involved in the nucleophilic catalysis step.

The second proof derives from the results obtained by experiments with inorganic phosphate-$H_2{}^{18}O$ oxygen exchange. These also demonstrate that an *E*-P covalent intermediate is

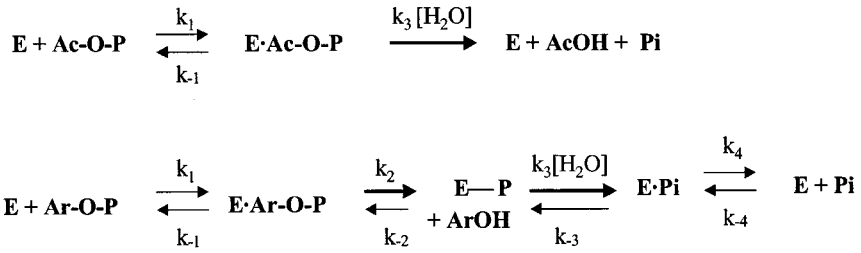

SCHEME 3. **Two different pathways for acyl phosphate (*top*) and aryl phosphate (*bottom*) hydrolysis by ACP.** *E*, enzyme; *Ac*, acyl; *Ar*, aryl; *P*, phosphate group.

formed in the catalytic pathway (Fig. 2). Indeed, the inorganic phosphate-$H_2{}^{18}O$ oxygen exchange can occur only if an *E*-P covalent intermediate is formed and is hydrolyzed by cycling the two terminal step in the overall catalytic process shown in Scheme 2. The mutation of His-25 to Gln eliminates the capacity of the enzyme to catalyze the inorganic phosphate-$H_2{}^{18}O$ oxygen exchange (Fig. 2*D*), suggesting that a phosphohistidine is involved in the process.

The third proof comes from the Brønsted free energy relationship experiments. For different aryl phosphates, the Brønsted plot of k_{cat} *versus* the leaving group pK_a shows effectively constant k_{cat} values (Fig. 3, *right*), indicating that a common intermediate is formed before the rate-limiting step of the catalytic pathway (see Scheme 1). The slope of the curve is slightly negative, giving a β_{1g} value close to zero (−0.07). This value indicates that a very low amount of negative charge develops on the leaving group oxygen in the transition state. A flat leaving group dependence suggests two hypotheses: either the protonation of the leaving group occurs at the transition state by general acid catalysis, or alternatively, the hydrolysis step that leads to the release of phosphate is not rate-limiting. The latter hypothesis is ruled out because CT-ACP is able to catalyze transphosphorylation from pNPP to glycerol; only if the *E*-P covalent complex (Scheme 1) accumulates before the rate-limiting step can the addition of a nucleophile (glycerol) competing with water increase the overall substrate breakdown (Table I).

In contrast with the results on aryl phosphates, previous findings on acyl phosphates (24) have demonstrated that the structure of the acyl group can have a dramatic effect on the rate of CT-ACP catalysis (β_{1g} value of −1.38). The difference of 1.34 units of the leaving group pK_a for acetyl phosphate (4.75) and *p*-nitrobenzoyl phosphate (3.41) leads to a 50-fold enhancement of k_{cat} for *p*-nitrobenzoyl phosphate *versus* acetyl phosphate (24). Considering both substrate types (acyl phosphates and aryl phosphates), a break in the leaving group dependence (see Fig. 3) is usually attributed to a change in either the mechanism or the rate-limiting step. The results of our experiments support the former. Indeed, the earlier model for the hydrolysis mechanism of acyl phosphates by CT-ACP, based on x-ray crystallography data, does not include any step of nucleophilic catalysis (12). The mechanism proposed by Thunnissen *et al.* (12) also agrees with our results because we observed no transphosphorylation from benzoyl phosphate to glycerol, consistent with the absence of any *E*-P covalent intermediate in the catalytic pathway of acyl phosphate hydrolysis.

Collectively, all of our findings suggest that CT-ACP-catalyzed hydrolyses of the two kinds of substrates follow two different pathways (as shown in Scheme 3).

For acyl phosphates, a nucleophilic water molecule attacks the Michaelis complex directly, producing P_i and the carboxylate anion. On the contrary, for aryl phosphates, the nucleophilic His-25 attacks the phosphorus atom of the substrate in the Michaelis complex, phosphorylating the enzyme. The hydrolysis of the *E*-P covalent complex concludes the process and is rate-limiting. The difference among the two mechanisms could depend on the fact that the carboxylate anion is a better leaving group than the phenolate anion. For acyl phosphates, this may favor the formation of a strongly dissociative transition state in the limiting step (as indicated by the strong dependence of k_{cat} on the leaving group pK_a; see Fig. 3, *left*), which is efficiently stabilized by the active site environment. This conclusion is supported by previous findings obtained for the strictly homologous bovine CT-ACP (about 90% sequence identity), which show that the formation of the transition state during benzoyl phosphate hydrolysis is accompanied by a strong reduction in the entropy of the hydrated enzyme-transition state complex compared with that of the hydrated enzyme-substrate Michaelis complex (24).

The binding of ACP to pNPP is not influenced by the H25Q mutation; at pH 5.3 we found K_m = 1.03 ± 0.13 mM for the mutant and a K_m = 1.10 ± 0.04 mM for the wild-type enzyme. In contrast, the binding of ACP to benzoyl phosphate is significantly affected by the His-25 mutation; at pH 5.3, we found K_m = 0.55 ± 0.03 mM for the mutant and K_m = 0.16 ± 0.01 mM for the wild-type enzyme. Furthermore, the mutation H25Q causes a significant decrease in the specificity constant k_{cat}/K_m for both pNPP and benzoyl phosphate. These findings indicate that His-25 is involved in the catalysis of both kinds of substrates, although the results reported in this study suggest that this residue plays different roles in the two different pathways. These and other findings, such as the observation that aryl phosphates behave as competitive inhibitors with respect to acyl phosphates (data not shown), collectively demonstrate that the enzyme possesses a unique active site. The unusual behavior of CT-ACP with regard to the mechanism of hydrolysis of two different kinds of substrates could be related to the strongly different chemical properties of the leaving groups (carboxylate and phenolate), which favor the formation of different transition states in the respective chemical steps of the catalytic hydrolysis processes. Results from the Brønsted analysis of acylphosphatase-catalyzed reactions (Fig. 3) clearly indicate a change in the nature of the transition state with a change the nature of the substrates. We think that for acyl phosphates, the intrinsic high stability of the carboxylate anion leaving group in the transition state is the driving force of the hydrolytic reaction, whereas for aryl phosphate monoesters a proton must be donated to the leaving group in the transition state for a productive forward reaction.

Previously, we demonstrated that Woodward's reagent K (*N*-ethyl-5-phenylisoxazolium-3′-sulfonate) is able to form a Michaelis-like complex with human CT-ACP and then inactivate the enzyme modifying His-25 (25). Woodward's reagent K interacts with the substrate binding site by its sulfonic group moiety, as suggested by the fact that some competitive inhibitors elicit protective actions against inactivation. The chemical modification of His-25 by Woodward's reagent K is relatively fast and highly specific, because other residues in the ACP molecule were not modified (25). The fact that Woodward's reagent K, which behaves as a substrate-like compound, binds to the CT-ACP active site and reacts easily with His-25 agrees with the presence of this strongly reactive nucleophilic residue

in the active site environment. In fact, His-25 is very close to Arg-23, an essential residue involved in substrate binding (12).

The cellular function of acylphosphatase is still under debate. In our opinion, the most interesting results on the physiological function of the enzyme in metazoan organisms are those demonstrating its capability of uncoupling the membrane ion pumps acting on the aspartyl phosphate intermediate formed during their functions. Nevertheless, the enzyme seems to be implicated in other processes such as differentiation and apoptosis (4–6). Transient expression of ACP in cells induces apoptosis (26), and thus it has been hitherto impossible to obtain stable clones overexpressing the enzyme. An understanding of all of the aspects of the action mechanism of acylphosphatase may help in the design and construction of specific enzyme inhibitors useful for revealing the true substrates of acylphosphatase in differing cell types and thus toward discovering its function.

Acknowledgments—We thank Gloria Borgogni for technical support. We are also indebted to Drs. Gloriano Moneti and Giuseppe Pieraccini of the "Centro Interdipartimentale di Servizi di Spettrometria di Massa," University of Florence, Italy.

REFERENCES

1. Nediani, C., Marchetti, E., Nassi, P., Liguri, G., and Ramponi, G. (1991) *Biochem. Int.* **24,** 959–968
2. Nassi, P., Nediani, C., Liguri, G., Taddei, N., and Ramponi, G. (1991) *J. Biol. Chem.* **266,** 10867–10871
3. Cecchi, C., Liguri, G., Pieri, A., Degl'Innocenti, D., Nediani, C., Fiorillo, C., Nassi, P., and Ramponi, G. (2000) *Mol. Cell. Biochem.* **211,** 95–102
4. Berti, A., Degl'Innocenti, D., Stefani, M., and Ramponi, G. (1992) *Arch. Biochem. Biophys.* **294,** 261–264
5. Chiarugi, P., Raugei, G., Marzocchini, R., Fiaschi, T., Ciccarelli, C., Berti, A., and Ramponi, G. (1995) *Biochem. J.* **311,** 567–573
6. Chiarugi, P., Degl'Innocenti, D., Taddei, L., Raugei, G., Berti, A., Rigacci, S., and Ramponi, G. (1997) *Cell Death Differ.* **4,** 334–340
7. Raugei, G., Degl'Innocenti, D., Chiarugi, P., Solito, E., Modesti, A., and Ramponi, G. (1999) *Biochem. Mol. Biol. Int.,* **47,** 127–136
8. Chiarugi, P., Degl'Innocenti, D., Raugei, G., Fiaschi, T., and Ramponi, G. (1997) *Biochem. Biophys. Res. Commun.* **231,** 717–721
9. Raugei, G., Modesti, A., Magherini, F., Marzocchini, R., Vecchi, M., Ramponi, G. (1996) *Biotechnol. Appl. Biochem.* **23,** 273–278
10. Taddei, N., Stefani, M., Vecchi, M., Modesti, A., Raugei, G., Bucciantini, M., Magherini, F., and Ramponi, G. (1994) *Biochim. Biophys. Acta* **1208,** 75–80
11. Taddei, N., Stefani, M., Magherini, F., Chiti, F., Modesti, A., Raugei, G., and Ramponi, G. (1996) *Biochemistry* **35,** 7077–7083
12. Thunnissen, M. M. G. M., Taddei, N., Liguri, G., Ramponi, G., and Nordlund, P. (1997) *Structure* **5,** 69–79
13. Camici, G., Manao, G., Cappugi, G., and Ramponi, G. (1976) *Experientia* **32,** 535
14. Zhang, Z. Y., and Van Etten, R. L. (1991) *J. Biol. Chem.* **266,** 1516–1525
15. Fiaschi, T., Raugei, G., Marzocchini, R., Chiarugi, P., Cirri, P., and Ramponi, G. (1995) *FEBS Lett.* **367,** 145–148
16. Deng, W. P., and Nickoloff, J. A. (1992) *Anal. Biochem.* **200,** 81–88
17. Sanger, F., Nicklen, S., and Coulson, A. R. (1977) *Proc. Natl. Acad. Sci. U. S. A.* **74,** 5463–5467
18. Ramponi, G., Treves, C., and Guerritore, A. (1966) *Experientia* **22,** 705–706
19. Baginski, E. S., Foa, P. P., and Zak, B. (1967) *Clin. Chim. Acta* **15,** 155–158
20. Fersht, A. (ed) (1999) *Structure and Mechanism in Protein Sciences*, p. 216–244, W. H. Freeman and Co., New York
21. Zhao, Y., Wu, L., Noh, S. J., Guan, K. L., and Zhang, Z. Y. (1998) *J. Biol. Chem.* **273,** 5484–5492
22. Zhang, Z. Y., Malachowski, W. P., Van Etten, R. L., and Dixon, J. E. (1994) *J. Biol. Chem.* **269,** 8140–8145
23. Vincent, J. B., Crowder, M. W., and Averill, B. A. (1992) *Trends Biochem. Sci.* **17,** 105–110
24. Paoli, P., Cirri, P., Camici, L., Manao, G., Cappugi, G., Moneti, G., Pieraccini, G., Camici, G., and Ramponi, G. (1997) *Biochem. J.* **327,** 177–184
25. Paoli, P., Fiaschi, T., Cirri, P., Camici, G., Manao, G., Cappugi, G., Raugei, G., Moneti, G., Ramponi, G. (1997) *Biochem. J.* **328,** 855–861
26. Giannoni, E., Cirri, P., Paoli, P., Fiaschi, T., Camici, G., Manao, G., Raugei, G., Ramponi, G. (2000) *Mol. Cell. Biol. Res. Commun.* **3,** 264–270